Vibrational Coherence in Electron Donor−Acceptor Complexes

I. V. Rubtsov*,†,‡ and K. Yoshihara*,†

Japan Advanced Institute for Science and Technology, Hokuriku, Tatsunokuchi 923-1292, Japan, and Institute for Chemical Physics Research, Chernogolovka, Moscow Region 142-432, Russia

Received: June 17, 1999; In Final Form: August 18, 1999

The excited-state dynamics of several electron donor−acceptor complexes were studied by a femtosecond fluorescence up-conversion technique. The spontaneous fluorescence decay of the complexes contains an oscillatory component superimposed with a ultrafast decay component. The oscillations in fluorescence are observed for the complexes with three different electron acceptors, tetracyanoethylene (TCNE), chloranil, and fluoranil, with various electron donors, hexamethylbenzene, carbazole, 1-chloronaphthalene, *N*-methylaniline, and some others. The similar oscillatory frequencies are observed for the complexes with different donors and a common acceptor: ∼155 cm^{-1} (period of ∼215 fs) for complexes with TCNE, 178 cm^{-1} (187 fs) for the complexes with chloranil, and 212 cm^{-1} (157 fs) for the complex with fluoranil. The assignment of the oscillatory component to a particular vibration is proposed. It is concluded that the out-of-plane vibrational mode of the acceptor, having b_{3u} symmetry, is responsible for the observed oscillations in all three cases (three acceptors). The time-dependent fluorescence spectrum for the TCNE−HMB complex is reconstructed from the fluorescence dynamics at different wavelengths, and the fluorescence peak shift correlation function is obtained. The ultrafast relaxation of the fluorescence peak position is superimposed with the oscillatory component. The main component of the spectral relaxation of 115 fs is attributed mostly to the intramolecular vibrational energy redistribution process in both donor and acceptor parts of the complex. The oscillatory component of the fluorescence peak position demonstrates the modulation of the transition frequency during the vibrations. The modulation of the mean transition moment is observed as well. Thus, two mechanisms are observed to be responsible for the oscillations: the modulation of the transition frequency and the modulation of the mean transition moment by the vibrational motion.

1. Introduction

The development of femtosecond lasers made it possible to coherently excite vibrational motions in molecules. If an excitation pulse is shorter than a vibrational period, vibrations are excited coherently. Coherently excited vibrations could be observed by spectroscopic methods in real time as oscillations,[1−22] and specific knowledge could be obtained about dynamics of the particular vibrational mode.

Early reports of the vibrational coherence were on diatomic molecules in the gas phase,[2,3] where only one vibrational frequency is involved. Later, the coherent oscillations were observed in polyatomic molecules.[5−14] Recently, it was demonstrated that even in complex biological systems in proteins the complicated coherent motions with different frequencies could be observed.[16,18−20] Despite large progress in investigation of these complicated systems, the assignment of the coherence to particular vibrational modes is not unambiguous.

In this paper, we report the vibrational coherence in systems with medium complexity. These are various electron donor−acceptor (EDA) complexes formed by relatively large organic molecules in the liquid phase. Even though such complexes have many inter- and intramolecular vibrational modes, the underdamped oscillations with only one frequency are dominantly observed.[12−14,22] Upon photoexcitation to the charge-transfer band of a "weak" EDA complex, an electron is transferred from the HOMO orbital located mainly on the donor to the LUMO orbital located mainly on the acceptor molecule.[23,24] So the absorption of a photon is accompanied by the electron transfer from a donor to an acceptor. When a molecular system undergoes an electron-transfer reaction, the equilibrium positions of the nuclei of both reacting molecules change. In the case of photoexcitation of the EDA complex to its charge transfer (CT) band, the charge transfer occurs at the equilibrium geometry of the ground (almost neutral) state of the complex. Thus, after excitation of the complex, the ionic state is prepared which has to relax to the equilibrium geometry corresponding to the almost ionic state. As a result, different vibrations are excited in the complex. Surprisingly, only one oscillating frequency has been experimentally observed in EDA complexes.[12,14,22] The assignment of even this one vibration is not clear yet.

The EDA complex of HMB and TCNE has recently been studied by different methods of femtosecond spectroscopy.[12,14,22] In the transient absorption experiment, the oscillation with the frequency of 162 cm^{-1} excited by impulsive stimulated Raman scattering was observed in a bleach recovery signal.[12] As the bleach recovery signal is mainly determined by the absorption of the ground electronic state of the complex, the oscillation was assigned to the vibration in the *ground* state. A peak at about 163−165 cm^{-1} was observed in the resonance Raman spectrum of the complex.[25−28] An oscillation was recently observed in spontaneous fluorescence with the frequency of about 155 cm^{-1}.[14,22] As spontaneous fluorescence reflects only the excited-state properties, the oscillation in this case belongs to a coherent vibration in the *excited* electronic state of the

* Corresponding author. E-mail: ivr@jaist.ac.jp; yosihara@jaist.ac.jp.
† Japan Advanced Institute for Science and Technology.
‡ Institute for Chemical Physics Research.

10.1021/jp991998r CCC: $18.00
Published on Web 10/04/1999

complex. The oscillation frequencies observed in three types of experiments (resonance Raman, transient absorption, and fluorescence spectroscopies) are very similar and were tentatively assigned to the *inter*molecular vibrational mode either in the ground or in the excited states. The frequencies of the *inter*molecular vibrations are expected to be vastly different in the ground and excited states due to a large Coulombic attraction in the excited state of EDA complexes as the excited state is ionic and the ground state is almost neutral. This makes the assignment of the observed oscillations to the intermolecular stretching mode questionable.

In this paper, we present new experimental data for various complexes and discuss the assignment of the observed oscillations to a particular vibrational mode in the EDA complexes. The structure of the paper is as follows. The descriptions of the fluorescence up-conversion setup, the experimental conditions, and the procedures for data analysis are presented in the experimental part. The results are separately described for complexes with different acceptors used and consists of three parts: complexes with TCNE, chloranil, and fluoranil as acceptors. The assignment of the oscillating component and description of the fast decay component is presented in the discussion part.

2. Experimental Section

2.1. Time-Resolved Fluorescence Measurements. The femtosecond fluorescence up-conversion setup was described elsewhere.[29] Briefly, an all-solid-state cavity damped chromium−forsterite laser was used as a source of short light pulses (wavelength around 1270 nm, pulse duration of 55 fs). The second harmonic (SH) pulses generated by a β-barium borate (BBO) crystal were compressed by a prism pair compressor to 44 fs and used for excitation of the sample. The central wavelength of the laser could be tuned resulting in tuning of the SH central wavelength from 610 to 655 nm. The fluorescence was gated by the fundamental pulses passed through an optical delay line. An up-converted light at sum frequency produced by a type-I BBO up-conversion crystal is spectrally selected and measured by a photomultiplier working in a photon counting regime. The instrument response function measured as a time-resolved Raman scattering from a pure solvent is down to 75 fs (fwhm) for excitation wavelengths from 622 to 640 nm and about 85−90 fs for the edges of the tuning range. The sample was circulated in a fused silica flow cell with 0.5 mm optical thickness and 0.7 mm thickness of the walls. The whole setup was optimized for the highest time resolution.

2.2. Chemicals and Sample Preparation. Hexamethylbenzene (HMB) 99%, 1-chloronaphthalene (ClNP), 90%, *N*-methylaniline (MAN), 98%, dichloromethane (DCM), >99%, chloroform, >99%, carbon tetrachloride (CCl_4), 99.8% from Wako Pure Chemical Industries, Ltd., chloranil (tetrachloro-1,4-benzoquinone) 99%, fluoranil (tetrafluoro-1,4-benzoquinone) 97% from Aldrich, tetracyanoethylene (TCNE), >98%, bromanil (tetrabromo-1,4-benzoquinone), >98% from Tokyo Kasei Organic Chemicals Co., Ltd., carbazole, >97%, from Kanto Chemical Co., Inc., and perdeuterated hexamethylbenzene-d_{18} (HMB-d_{18}), 98.1 atom % of D from CDN Isotopes were used as received. A sketch of the donors and acceptors used in this work is shown in Figure 1.

Concentrations of the complexes were chosen to give the optical density of about 0.3 (or a bit smaller) in a 0.5 mm sample cell. At the same time, concentrations were kept so that mostly 1:1 complexes were formed. While in solvents with moderate polarity (CH_3Cl and DCM) mostly 1:1 complexes are formed,

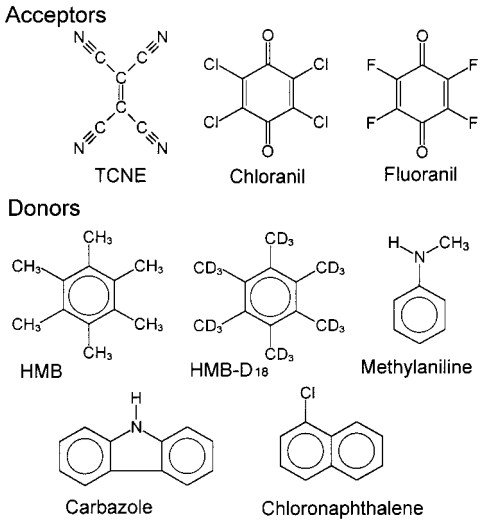

Figure 1. Donors and acceptors used in this work.

in CCl_4, a special care was taken to avoid 2:1 complex formation. For the complexes of TCNE with HMB in CCl_4, experiments were made with concentrations of TCNE ~6 mM and HMB ~30 mM which yield 18% of the 2:1 complexes (using equilibrium constants $K_1 = 151\ M^{-1}$ and $K_2 = 7.3\ M^{-1}$ and extinction coefficients $\epsilon_1 = 4613\ M^{-1}\ cm^{-1}$ and $\epsilon_2 = 6770\ M^{-1}\ cm^{-1}$ [27,30,31]). The equilibrium constant K_1 strongly depends on the solvent used. It is 20.7 M^{-1} in DCM and about 300 M^{-1} in cyclohexane.[31]

2.3. Data Analysis and Spectral Reconstruction. The fluorescence data were fitted by the function $f(t)$ (eq 1) convoluted with the instrument response function. As an instrument response, the time-resolved Raman scattering signal from pure DCM was used.

$$f(t) = A_1 \exp(-t/\tau_1) + A_2 \exp(-t/\tau_2) + A_3 \cos(\omega t + \varphi) \exp(-t/\tau_{damp}) \quad (1)$$

Here, ω is the frequency of oscillation, φ is the initial phase, and τ_{damp} is the damping time of the oscillation. For a spectral reconstruction, the fluorescence decays were normalized according to the time integrated spectrum obtained from ref 28. The differences in fluorescence decay at different wavelengths could be observed up to ~5 ps, whereas the main difference happens in 0.5 ps (more then 75% of the decay; see Figure 2). After 5 ps delay, the fluorescence decays synchronously at all wavelengths and reflects only the lifetime of the excited state of the complex, which is much longer (about 13 ps[12,14]) than the spectral relaxation times. So the amplitudes of fluorescence decays at 5 ps (not time integral) were normalized according to the steady-state fluorescence intensity at the same wavelength. The estimated error caused by normalization using the amplitude at 5 ps but not integral is less than 5%. We used this type of normalization since the integration of the tails, which are rather noisy in the red part of the spectrum, gives a larger error. After normalization, the time-dependent spectra were constructed. Each spectrum was fitted with a Gaussian function, and the wavelength of the spectral maximum was determined from the fit. Deconvolution of the individual fluorescence signals was not performed for the spectrum reconstruction.

2.3.1. Semiempirical Calculations. The molecular structures in the gas phase were modeled by the Hyperchem software, employing a molecular orbital theory with parametrized model 3 (PM3) Hamiltonians. For optimization of the configurations of the closed-shell molecules (neutral molecules), the restricted

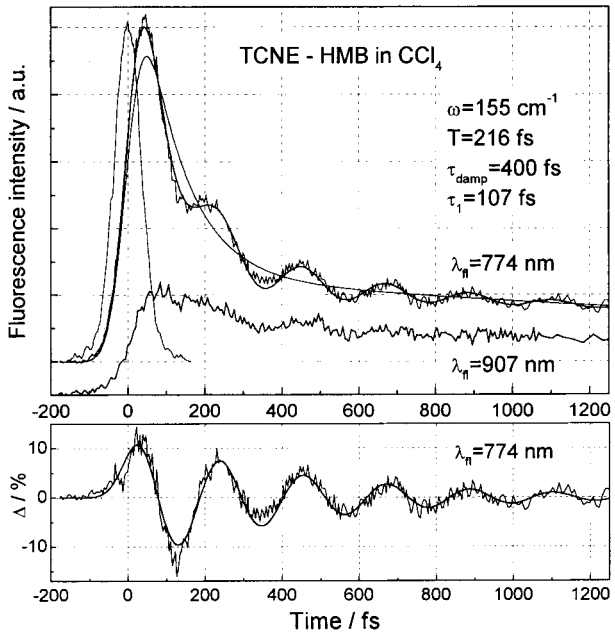

Figure 2. Fluorescence decays of the TCNE−HMB complex in CCl_4 at 774 and 907 nm. The best fit of convolution of $f(t)$ function with instrument response function is shown. Instrument response function of 85 fs (fwhm) used for the convolution is also shown. The oscillatory component for the signal at 774 nm is emphasized separately at the bottom.

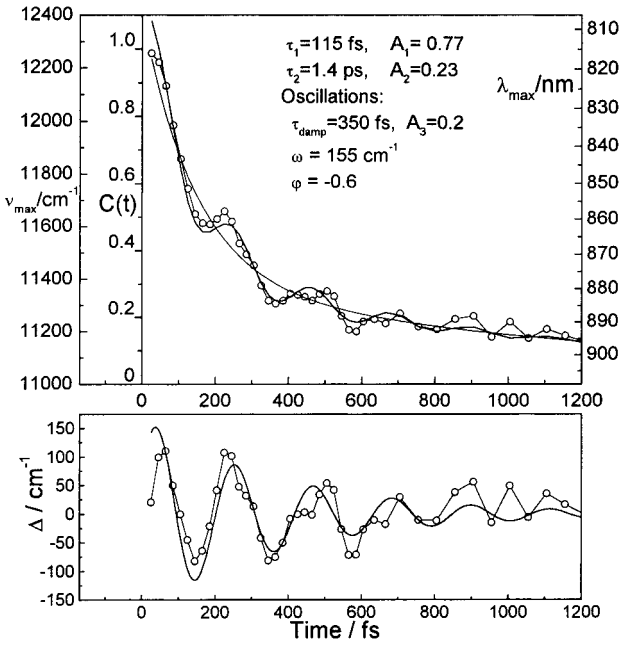

Figure 3. Maximum of fluorescence spectrum $\nu(t)$ time behavior. The normalized spectral shift correlation function $C(t) = [\nu(t) - \nu(\infty)]/[\nu(0) - \nu(\infty)]$ is shown as additional Y axis. The oscillating component determined as a difference between experimental data and fit with eq 1 where the oscillating component was set to zero is shown at the bottom. The best fit parameters are $\tau_1 = 115$ fs, $A_1 = 0.77$, $\tau_2 = 1.4$ ps $A_2 = 0.23$, $\tau_{damp} = 350$ fs, $A_3 = 0.21$, $h\omega = 155$ cm^{-1}, $\varphi = -0.6$.

Hartree−Fock (HF) method was used, while for the open-shell molecules (ions), the unrestricted HF method was used. The PM3 semiempirical method was used for the normal-mode analysis.

3. Results

3.1. Oscillations in TCNE−HMB Complex. The EDA complex in which oscillations were found for the first time was the complex between TCNE and HMB.[12,14] The charge-transfer band of the steady-state absorption spectrum of the complex is broad (width at half-maximum of ∼5500 cm^{-1}) with a maximum at 537 nm in CCl_4. The time-integrated fluorescence spectrum is also broad (∼4100 cm^{-1}) with a maximum at 917 nm[26,28] with a very large Stokes shift of about 7500 cm^{-1} in CCl_4. Recently, we reported the oscillations observed in spontaneous fluorescence from this complex.[14] In this paper, we present new experiments with a wider spectral range of fluorescence observation from 700 nm (which in a very "blue" side of the time-integrated fluorescence spectrum) to 970 nm (which is "redder" than the fluorescence maximum). The example of the fluorescence decay measured at 774 nm is presented in Figure 2. The instrument response function obtained by measuring the time-resolved Raman scattering from pure solvent is shown in the same figure. The best fit obtained as a convolution of the $f(t)$ function (eq 1) with the instrument response function is also shown. The oscillating component is emphasized in the lower graph. One can see a clear oscillation of the fluorescence intensity with a time period of 216 fs which corresponds to the frequency of 155 cm^{-1}. Oscillations with the same frequency were observed for eight wavelengths from 700 to 895 nm. At 907 nm, the oscillatory component is observable (Figure 2), but it cannot be fitted well with a single sinusoidal function. Another frequency seems to be involved in the initial part of the signal. Generally, at the wavelengths near the fluorescence maximum, a twice higher frequency is expected to be involved as a wave packet passes the maximum of the fluorescence spectrum twice in one period.[32,33] But the 2ω frequency was not clearly observed due probably to the small amplitude of oscillations expected in the region of the fluorescence maximum[34] and/or a lack of the time resolution.

A fast exponential decay component is superimposed with oscillations. It decays with the characteristic time of about 100 fs at the "blue" edge of fluorescence spectrum and has a spectral diffusion character[14] (Figure 2). The amplitude of this component decreases, and the characteristic decay time increases with increasing the wavelength of observation from 700 to 970 nm. This component was assigned to a vibrational relaxation,[14] as the excess of the photon energy above the 0−0 transition is rather large (about 1800 cm^{-1}). The spectral change in time is characterized by constructing of the peak-shift correlation function $C(t)$, as described below. Although the evolution of $C(t)$ has mainly been used to characterize the solvent dynamics,[35−38] it is generally related to all kinds of the spectral relaxation. On the fast time scale, the vibrational relaxation and/or intramolecular vibrational energy redistribution (IVR) contribute to $C(t)$ (see section 4.1). These processes are expected to be predominant especially in nonpolar solvents where solvation effect is small.

3.2. Reconstruction of Fluorescence Spectrum. The time-dependent fluorescence spectra were constructed according to the procedure described in the Experimental Section. The time behavior of the peak position of the fluorescence spectrum is shown in Figure 3. The normalized peak shift correlation function $C(t)$ is determined as

$$C(t) = \frac{\nu(t) - \nu(\infty)}{\nu(0) - \nu(\infty)} \tag{2}$$

where $\nu(t)$ and $\nu(0)$ are the wavenumbers of the peak position of the fluorescence spectrum at times t and zero, respectively, and $\nu(\infty)$ is the fluorescence maximum at infinite time, which was taken as a maximum of the time-integrated fluorescence

TABLE 1: Parameters of the Complexes Studied in This Work

donor	acceptor	solvent	abs λ_{max}, nm	observed λ_{fl}, nm	$\tau_{damp.}$, fs	$\omega_{oscill.}$, cm^{-1}
HMB	TCNE	CCl_4	535	700−970	350 ± 80	156 ± 3
HMB	TCNE	CH_2Cl_2	540	800−907	450 ± 50	155 ± 2
HMB(D_{18})	TCNE	CCl_4	535	770	300 ± 50	155 ± 3
carbazole	TCNE	$CHCl_3$	610	865	210 ± 50	153 ± 4
Cl−naphthalene	TCNE	CH_2Cl_2	∼565	700	280 ± 50	154 ± 4
HMB	chloranil	CH_2Cl_2	520	810, 850	400 ± 50	178 ± 4
MAN	chloranil	CCl_4	595	866	350 ± 50	179 ± 5
HMB	fluoranil	CH_2Cl_2	490	808	350 ± 50	212 ± 7

spectrum. $C(t)$ is shown in the same figure as a second Y axis. It consists of an exponential like relaxation with an oscillatory component. The relaxation is well fitted by a biexponential decay function with a fast component of 115 ± 25 fs (77%) and a slow component of 1.4 ± 0.5 ps (23%). These exponential decay components will be discussed in detail in section 4.1. The frequency of oscillations of 156 ± 5 cm^{-1} is the same frequency observed in the single wavelength measurements. So, the fluorescence spectral position is oscillating due to a wave packet motion in the excited state of the complex. In other words, some of the vibrational motion excited coherently by the light pulse modulates the transition frequency between the excited and ground states. We will further discuss a contribution to the observed oscillations from a modulation of the transition moment by molecular vibrations (section 4.8).

The oscillatory fluorescence of HMB−TCNE complex was observed not only in CCl_4 but also in DCM (Table 1). The frequency of oscillation (155 cm^{-1}) is the same as that observed in CCl_4 (156 cm^{-1}), while the damping time becomes clearly longer (about 350 fs in CCl_4 and about 450 fs in DCM). The longer damping time for DCM is probably related to the fact that frequencies of intramolecular vibrational modes of DCM are much smaller than that of CCl_4. The smallest frequency of CCl_4 is below 200 cm^{-1} (the highest is about 700 cm^{-1}), while that of DCM is about 300 cm^{-1} (the highest is about 3100 cm^{-1}). The lack of the intramolecular solvent modes with the frequencies similar to the oscillation frequency in the complex (∼155 cm^{-1}) decrease the dephasing rate for the vibration of the complex in DCM.

The oscillating component has either intermolecular or intramolecular origin. To specify which vibrational motion is responsible for the oscillation, we have performed experiments with different complexes. First, the complexes in which donors are varied and the acceptor is common (TCNE) have been studied (section 3.3). Second, the complexes with different acceptors have been investigated (sections 3.4 and 3.5).

3.3. Complexes of TCNE with Different Donors. *3.3.1. Deuteration of HMB.* To specify *inter*- or *intra*molecular origin of the oscillation, the experiment with perdeuterated HMB (HMB-d_{18}) was performed (Figure 4 and Table 1). Upon perdeuteration of the HMB, the reduced mass of the complex increases from 71.5 to 74.8 g/mol. Assuming an invariable force constant for the intermolecular vibration, it gives 2.2% decrease of the frequency of the intermolecular stretching mode. In the wavenumber representation, it corresponds to a 3.5 cm^{-1} decrease of the vibrational frequency. The results of the fits show no substantial difference in the frequencies in these two cases. Unfortunately, the experimental accuracy in frequency determination is similar to the difference to be observed. Even though the error bars of the absolute values of the frequency are comparable with the expected effect, the relative accuracy seems to be higher (considering the same "zero" time position in both experiments made on the same day). Taking this into account, the difference in the frequencies for these two cases

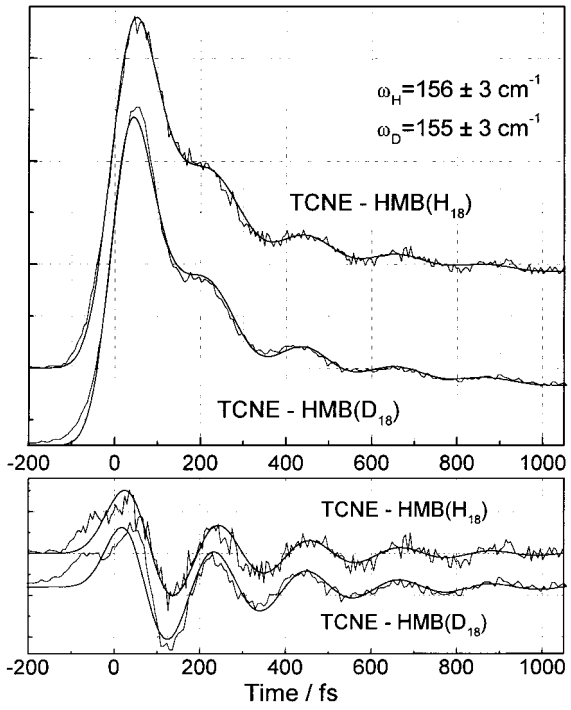

Figure 4. Fluorescence decays of the complexes of TCNE with normal HMB (H_{18}) and perdeuterated HMB (D_{18}) in CCl_4 at 770 nm. Oscillatory components are shown at the bottom.

(if any) seems to be smaller than 3 cm^{-1}. Thus, this experiment is not supporting the assignment of the frequency of the oscillations to the intermolecular stretching mode.

3.3.2. Complexes of TCNE with Carbazole and Chloronaphthalene. The underdamped oscillations of spontaneous fluorescence are observed in different complexes: carbazole−TCNE (Table 1) and chloronaphthalene−TCNE (Figure 5). The frequencies of the oscillations in these complexes (153 ± 4 cm^{-1} with carbazole and 154 ± 4 cm^{-1} with chloronaphthalene) are very similar to the frequency observed in HMB−TCNE complex, while the damping times and lifetimes of the excited state of the complexes vary significantly (Table 1). We cannot completely eliminate a possibility that the intermolecular frequencies of the different complexes accidentally coincide, but such probability looks negligible. Thus, the experiments with different donors are also not in favor to attribute the oscillating mode to the intermolecular stretching mode.

It should be noted that while for the complexes of TCNE with perdeuterated HMB and nondeuterated HMB the same force constant could be considered and donor mass dependence of the intermolecular frequency is expected. If different donors are used to form complexes with TCNE, the force constant varies substantially as the equilibrium constant of complex formation changes for about 2 orders of magnitude. This makes it difficult to predict how the intermolecular vibrational frequency depends on the donors masses. The oscillatory behavior was observed in several other EDA complexes with

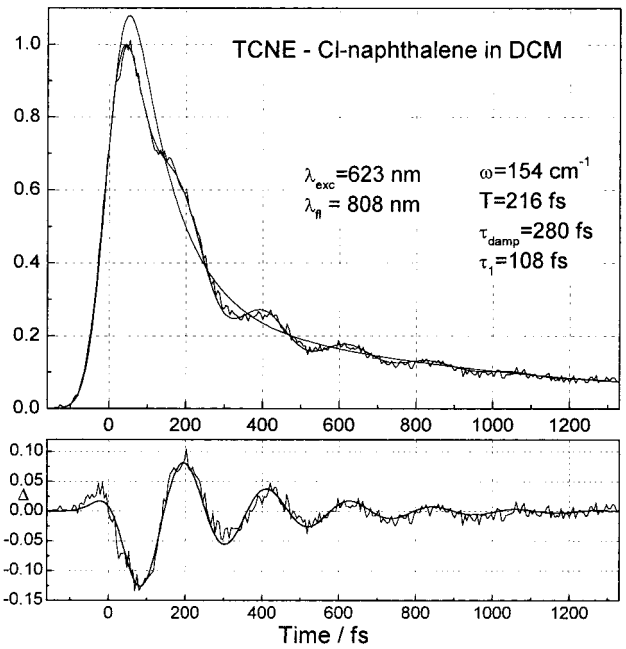

Figure 5. Fluorescence decay of TCNE−chloronaphthalene complex in DCM observed at 808 nm and the best fit of convolution with instrument response function is shown. Extracted oscillatory component is shown below.

different acceptors. These are complexes with chloranil and fluoranil as acceptors.

3.4. Oscillations in Chloranil−HMB and Chloranil−MAN Complexes. The fluorescence decays of the chloranil−HMB complex in DCM at two different wavelengths of observation are shown in Figure 6. Clear underdamped oscillations are observed, although the amplitude of the oscillations is about 3 times smaller than that for the complexes with TCNE. For both wavelengths of observation at 810 and 850 nm, there is only one dominant oscillatory frequency of 178 ± 4 cm^{-1} (period of oscillations of 188 fs) which is about 23 cm^{-1} higher than the frequency in the complexes with TCNE.

Oscillations were also observed in fluorescence from the complex of chloranil with *N*-methylaniline (MAN) (Figure 7). The oscillatory frequency of 179 ± 4 cm^{-1} (186 fs period) is similar to that for the chloranil−HMB complex (Table 1).

The oscillations in fluorescence of both complexes with chloranil as an acceptor have similar features: same oscillatory frequency, similar amplitude of oscillations even though the absorption maxima of the complexes are rather different (520 nm for chloranil−HMB and 595 nm for chloranil−MAN; see Table 1).

3.5. Oscillations in Fluoranil−HMB Complex. Finally, oscillations in fluoranil−HMB complex in DCM are observed (Figure 8). The oscillation period is 157 fs which corresponds to the frequency of 212 ± 7 cm^{-1} (Table 1). The amplitude of oscillations is small. It is partly limited by the time resolution. Several other complexes were studied including bromanil−HMB and TCNQ−HMB, but no oscillations were detected while the fluorescence intensity is strong enough.

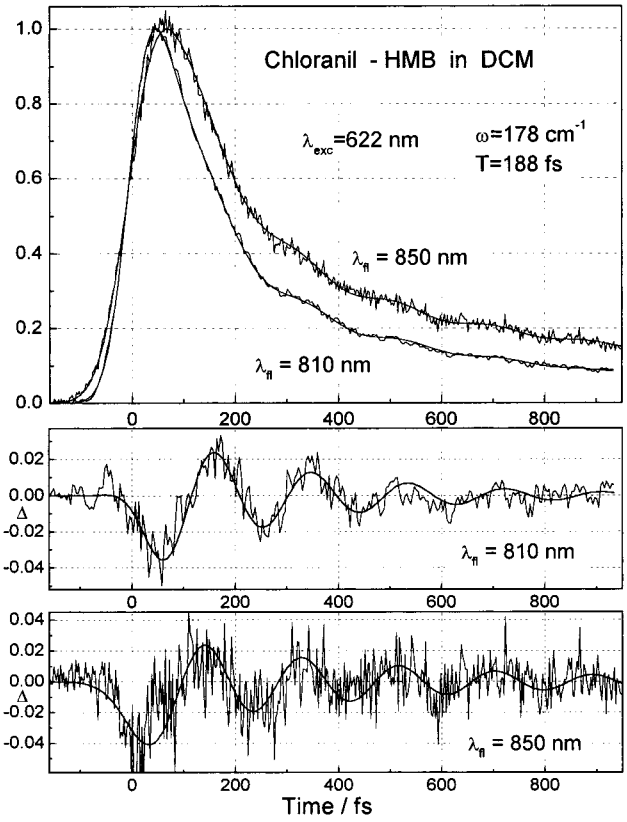

Figure 6. Fluorescence decays of chloranil−HMB complex in DCM at two observation wavelengths (810 and 850 nm) are shown with the best fits. The oscillatory components at both wavelengths are emphasized at the bottom.

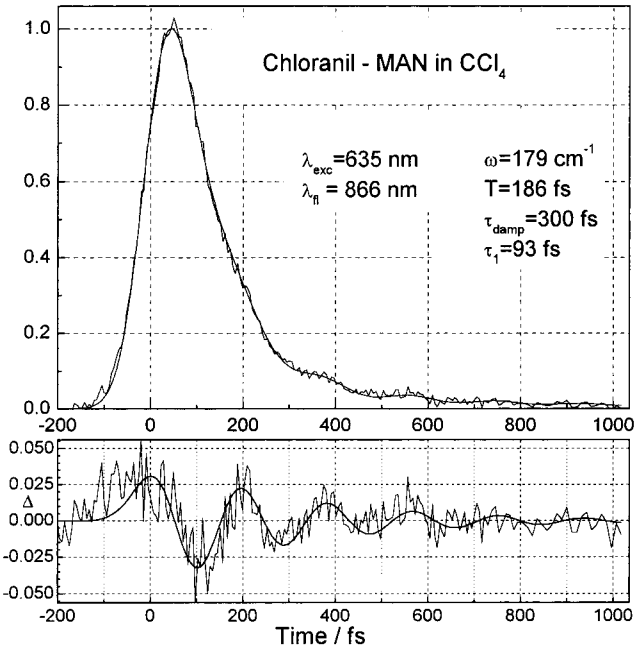

Figure 7. Fluorescence decay of chloranil−MAN complex in CCl_4 at 866 nm is shown with the best fit. Extracted oscillatory component is shown below.

4. Discussion

4.1. Vibrational Relaxation and IVR. The fast exponential decay component was observed in the fluorescence of all complexes studied. This component is due to vibrational relaxation (VR) and intramolecular vibrational energy redistribution (IVR) processes. In "weak" EDA complexes, an electronic excitation to the CT absorption band always causes excitation of different vibrations. Upon photoexcitation, the complex is "instantly" transferred from the mostly neutral form (D−A) to the mostly ionic form (D^+-A^-). At the Franck−Condon (FC) state, configurations of atomic skeleton of both D^+ and A^- correspond to the equilibrium configurations of

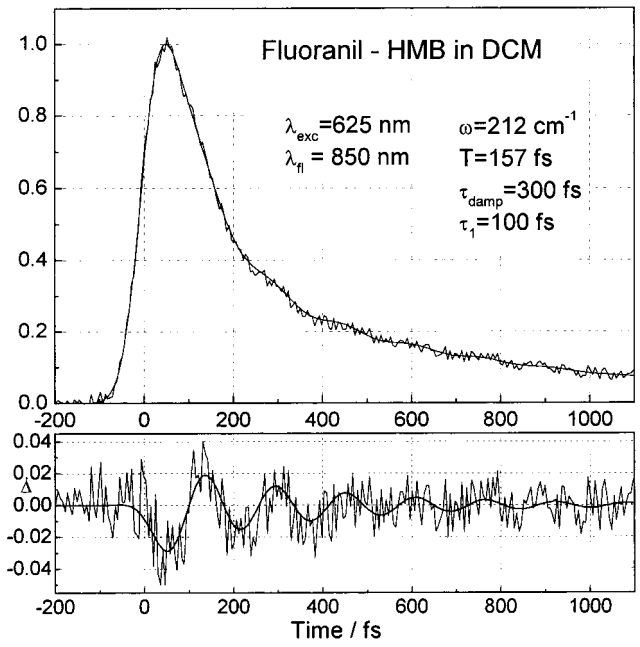

Figure 8. Fluorescence decay of fluoranil−HMB complex in DCM observed at 850 nm and the best fit of convolution with instrument response function is shown. Extracted oscillatory component is shown below.

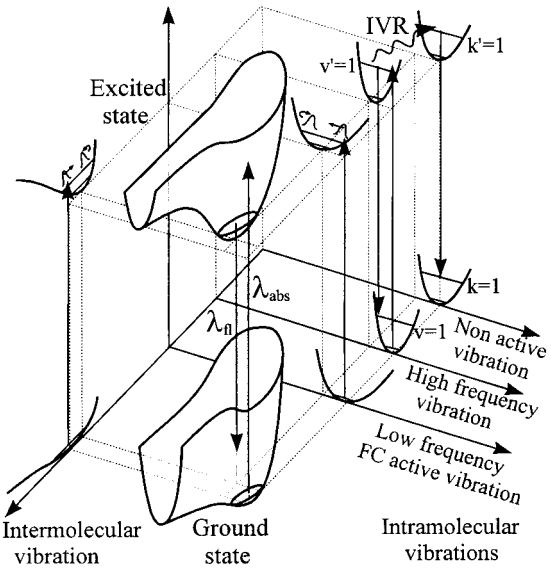

Figure 9. Schematic potential energy diagram. Projections to several vibrational modes of the multidimensional ground and excited potential energy surfaces are shown. The wave packet motion is excited in two low-frequency modes: inter- and intramolecular. IVR process is shown as an energy transfer from FC active mode to nonactive mode (see text for details).

neutral D and A. The equilibrium geometries of the ions D^+ and A^- are quite different from that of the neutral D and A. It means that by photoexcitation vibrations are excited in both D and A as nuclei have to reorganize in order to reach the equilibrium geometry of the products $(D^+-A^-)^*$. That is the reason that the CT band in EDA complexes is very broad and the Stokes shift is very large even in the gas phase.[39,40] The vibrational energy from vibrationally hot states can flow to the vibrations of smaller energy located in the same molecule (IVR process) and/or to rovibronic levels of the solvent (VR). The former process is considered to be faster than the latter, as a coupling between intramolecular modes is usually stronger than that of modes in different molecules (at least for relatively large molecules). The larger is a molecule, the larger is the density of states and the faster is the IVR process. It was found that IVR in the ground electronic state is much slower than that in the excited electronic state.[41,42]

It is obvious that vibrational relaxation (vibrational cooling) will cause a dynamic spectral shift of the fluorescence. To illustrate that IVR can cause the same effect, we consider a simple molecular system having two vibrational modes with similar frequencies; one is FC active and another is inactive. Let us also assume that, after photoexcitation of the FC active vibration in the excited electronic state, the vibrational energy is transferred from the FC-active to the inactive mode (IVR process). One can consider two projections of the ground (S_0) and excited (S_1) potential energy surfaces to these two vibrational coordinates (Figure 9). Note that there should be some shift of the equilibrium positions of S_1 and S_0 in the projection to the FC-active mode (v), while no shift (and no frequency change) is considered for the non-FC-active mode (k). By photoexcitation the $S_1(v'=1, k'=0)$ excited state is prepared. Initially, the emission wavelength is determined by the transition from $S_1(v'=1, k'=0)$ to $S_0(v=0, k=0)$. After energy transfer from the FC-active to nonactive vibration a state $S_1(v'=0, k'=1)$ is formed. In this case, the emission wavelength is determined by the transition from $S_1(v'=0, k'=1)$ to $S_0(v=1, k=1)$, since the $k'=1$ state on the S_1 surface is orthogonal to all other states in both electronic states except for $k = 1$ in the S_0 surface. The transition energy of the former is larger than that of the latter. The difference in energy corresponds to a vibrational quantum of the FC active vibration (if FC vibration is excited noncoherently). Thus the vibrational energy redistribution from the FC active vibrations to nonactive "dark" modes causes a dynamic "red" shift of the fluorescence spectrum.

Myers et al. analyzed the resonance Raman spectrum of the complex of HMB−TCNE and found that at least 11 vibrational modes are strongly contributing to the observed absorption and emission spectra.[25,26,28,43] Those are six vibrations of HMB (from 450 to 1570 cm^{-1}) as well as four vibrations of TCNE (from 542 to 2222 cm^{-1}). One low-frequency Raman-active vibration was observed at 165 cm^{-1}, which was tentatively assigned to the D−A stretching mode. Some of these FC-active modes are excited in our experimental conditions as the extra energy of the excitation photons is about 1800 cm^{-1} above the 0−0 transition. The high-frequency modes from 450 to 2222 cm^{-1} could not be excited and detected coherently based on time resolution of our setup. As we have shown above, migration of the vibrational energy to the solvent (VR) and to other "dark" modes in the complex (IVR) causes "red" shift of the emission spectrum in time. Since VR to solvent is expected to be much slower than IVR, the observed fast spectral shift (Figure 3) is assigned mostly to the IVR process, in particular, to energy transfer from the initially excited FC-active intramolecular modes of both D and A to the nonactive vibrational modes. We should emphasize that the solvent used is nonpolar solvent and solvation effect does not contribute much to the observed spectral shift. Two characteristic relaxation times of 115 ± 25 fs (77%) and 1.4 ± 0.5 ps (23%) of spectral relaxation were determined from the biexponential fit of peak shift correlation function $C(t)$ (Figure 3). The main component of 115 fs is assigned mainly to the IVR process, while the slow component might consist of different contributions: IVR, vibrational energy transfer to the solvent, and solvation. We should note that the value of 115 fs should be considered as an upper limit for the IVR process in this complex, as the single wavelength signals

were treated without deconvolution in the spectrum reconstruction procedure (see Experimental Section 2.3).

4.2. Oscillatory Component. As one can see from Figure 3, the fluorescence peak position of the complex does not only decay to the relaxed excited state but also oscillates during relaxation. The oscillating component is shown separately in the bottom graph of Figure 3. The frequency of oscillation is 156 ± 5 cm^{-1}, which is the same as that observed by the single wavelength observation. Thus, it can be seen that the transition frequency is modulated by some vibrational motion of the complex. There are several factors which determine the amplitude of the spectral modulation by vibrational motions. These are the displacement of the ground and excited state potential energy surfaces along the vibrational coordinate which causes oscillations and steepness of both potential energy surfaces along this coordinate. The larger are displacement and steepness, the greater is modulation of the transition moment during the vibration. Because of the large transition moment, these vibrations should contribute to the steady-state absorption and fluorescence spectra as a vibrational progression and should be potentially Raman-active vibrations.

Next, we will focus our attention on the assignment of the oscillating feature. Inter- and intramolecular modes will be examined. Experimental results can be summarized as follows. (1) The oscillating frequency is the same for the complexes with different donors when the acceptor, TCNE, is common. (2) It is different for complexes with different acceptors (TCNE, chloranil, and fluoranil). (3) It is the same for chloranil complexes with two different donors: HMB and MAN. (4) It is the same for the HMB−TCNE complex in different solvents.

These results suggest that the observed oscillatory frequencies belong probably not to the intermolecular D−A stretching mode but rather to the vibrational modes of the acceptors. In the following sections, we will consider the intramolecular vibrational modes of acceptors in detail. To be more accurate, we should consider the vibrational modes of the acceptor anion, as the excited states of the EDA complexes are ionic.[44] So, whenever data are available, we will discuss vibrational frequencies of both forms of acceptors: neutral and anion.

4.3. IR- and Raman-Active Modes in EDA Complexes. Let us consider that the line connecting centers of D and A is the axis of symmetry of the complex so that the complex belongs to the symmetry groups C_2 or C_{2v}. The C_{2v} group symmetry of the TCNE−HMB 1:1 complex was concluded by Liptay et al.[30] from electrooptical measurements (the C_{2v} group consists of one symmetry axis and two symmetry planes). In this case, the selection rules could be obtained for different vibrations to be active in Raman scattering or in IR absorption. For example, the A−D stretching mode will be Raman active as the vibration keeps the symmetry of the complex, while different modes belonging to the acceptor and the donor will be active either in IR or in Raman (or not active in both). In fact, all acceptors we used belong to the D_{2h} group symmetry,[45] so we will discuss here intramolecular modes of the acceptors in terms of this symmetry group. The vibrations, a_g, a_u, b_{3g}, and b_{3u} (of D_{2h} group), hold the symmetry of the complex, and b_{1g}, b_{2g}, b_{1u}, and b_{2u} do not hold. As we will see in part 4.4 there are two TCNE acceptor vibrational modes in the vicinity of 160 cm^{-1} to which observed oscillations could be assigned: to either the in-plane scissoring mode (b_{1u}) or the out-of-plane bending mode (b_{3u}) (Table 2 and Figure 10). With the assumption of the considered symmetry of the complex, b_{1u} should be IR active and b_{3u} should be Raman active in the complex.[46] In the acceptor (not in the complex), both modes should be IR active. Having these in mind, let us analyze what was observed in the IR absorption and Raman scattering experiments for TCNE, TCNE$^-$, and TCNE−HMB complex.

TABLE 2: Low-Frequency Ground State Vibrations of TCNE and TCNE−HMB Complex

species D_{2h}	frequencies of vibrations, cm^{-1} from ref 49[a]	PM3 calculations[b]	from ref 56[c]	description
a_u		72	101	torsion oop[d]
b_{2u}	103	112	127	(CN)−C−(CN) rocking
a_g	125	137	134	(CN)−C−(CN) scissoring
b_{3u}		167	170	(CN)−C−(CN) oop wag
b_{1u}	167	175	167	(CN)−C−(CN) scissoring
b_{3g}	278	293	291 or 305	(CN)−C−(CN) rocking

[a] Assignment of the TCNE modes based on experiment.[49] [b] Our semiempirical PM3 calculations of TCNE modes. [c] Normal vibrational modes in ref 56 were calculated for the TCNE−HMB complex, but the shown vibrations are located mainly on TCNE. [d] "oop" stands for out-of-plane modes.

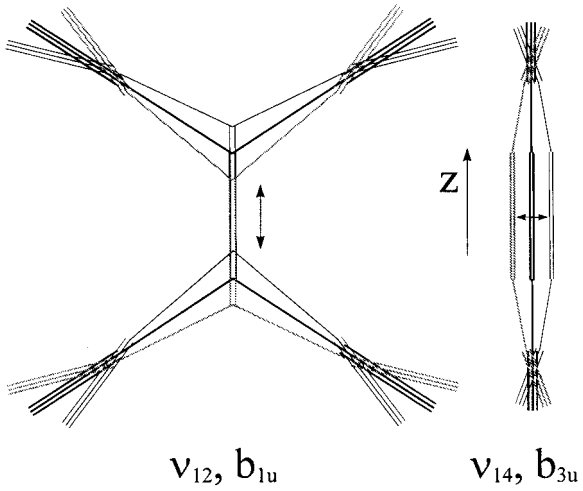

Figure 10. Illustration of the two normal modes of TCNE.

We should note that the assignment of low-frequency vibrations is not certain up to now, so the predictions made by semiempirical calculations will be used as well. For example, the out-of-plane vibration of the TCNE, ν_{14} (b_{3u}), was assigned only intuitively.[47]

4.4. Vibrations of TCNE and TCNE$^-$. The observed oscillatory frequency is about 155 cm^{-1} in the excited state of the TCNE complexes. We will assign it to intramolecular vibration of TCNE (or TCNE$^-$). There are two vibrations in TCNE with frequencies near the observed oscillatory frequency (Table 2). One is the scissoring mode (ν_{12}) having b_{1u} symmetry (D_{2h} point group, when the z axis is directed along the C═C band) and another is the out-of-plane bending mode (ν_{14}) with the b_{3u} symmetry (Figure 10). Both are the IR-active modes of TCNE. Three vibrational modes of 159, 166, and 180 cm^{-1} were observed in polycrystalline TCNE samples.[48] All three bands were assigned to ν_{12} (b_{1u}) ($C(CN)_2$ scissoring) without qualitative explanation for the reason of its splitting.[48] In the later work,[47] it was suggested that one of these three modes was the out-of-plane vibration ν_{14} (b_{3u}). The 180 cm^{-1} band was assigned to the ν_{14} mode and the 159 and 166 cm^{-1} modes were assigned to Davydov components of ν_{12}.[47] According to Michaelian et al., the 159 cm^{-1} band might alternatively be assigned to ν_{14}, but this would not leave any fundamentals to account for the 180 cm^{-1} band.[47] The far-IR spectrum of TCNE in the form of halocarbon mull was measured by Miller et al.[49] They observed

TABLE 3: Selected Vibrations of TCNE and TCNE$^-$

	experimental	calculations			
	$\nu_{(TCNE)}$/cm^{-1} from refs 47−49	$\nu_{(TCNE)}$ cm^{-1}	$\nu_{(TCNE^-)}$ cm^{-1}	species D_{2h}	description
ν_{12}	165	175	174	b_{1u}	in-plane scissoring
ν_{14}	(180)	167	148	b_{3u}	out-of-plane (CN)−C−(CN) wag

only one band at 165 cm^{-1} in the region under consideration and assigned it to the scissoring mode, ν_{12}.

Our semiempirical calculations give 175 cm^{-1} for b_{1u} and 167 cm^{-1} for b_{3u} modes (Table 3). The vibrational modes of TCNE anion were measured only from 200 cm^{-1} in IR absorption experiments.[50,51] According to our calculations (Table 3) and calculations of ref 50, there is almost no frequency shift of ν_{12} (b_{1u}) mode in anion relative to the neutral molecule. No data about ν_{14} (b_{3u}) mode in anion of TCNE were found. Our calculations suggest about 11% decrease of the ν_{14} frequency in TCNE anion compared to the neutral (Table 3). This reflects a decrease of a stabilization energy keeping the flatness of the molecule in TCNE anion and is a common feature for most of the out-of-plane modes of TCNE.

In the resonance Raman experiments[52] of the sodium and potassium salts of TCNE (in fact TCNE$^-$), the bands of ∼140, ∼160, and ∼170 cm^{-1} (with Na) or 175 cm^{-1} (with K) were observed. The assignment is complicated because of the different salt structures. Another complication is a possibility to assign these bands to lattice modes.

4.5. Raman Spectrum of the TCNE−HMB Complex. There are many studies on Raman spectroscopy of the TCNE−HMB complex.[27,28,43,53,54] While the high-frequency range is rather well characterized, the assignment of low frequencies is still uncertain. A strong Raman band in solution was observed at about 165 cm^{-1}.[27,28,43,53,54] The solvent dependence of this band is conflicting. Smith at al. observed it at 163 cm^{-1} in cyclohexane, 166 cm^{-1} in CCl_4, and 169 cm^{-1} in DCM,[27] while Kulinowski et al. reported the same frequency of 165 cm^{-1} for all these three solvents.[28,43] There is no consistency in the assignment of this band. Smith et al. assign it to an overtone of the D−A stretching mode ($2\nu_{DA}$)[27] based on the observation of Rossi et al.[48] that the 89 cm^{-1} peak belongs to the D−A stretching mode. Kulinowski et al. suggested that 165 cm^{-1} mode is the fundamental D−A stretching mode leaving a possibility to assign it to a scissoring mode of TCNE.[43] McHale et al. discussed several other possible assignments of this mode.[54] One of the possibilities is an IR-active acceptor mode which becomes Raman active in the complex, because a symmetry of the complex is lower than that of the acceptor. As a candidate, they considered the b_{1u} scissoring mode of TCNE, even though the b_{1u} mode is *nontotally* symmetric for the C_{2v} group symmetry of the complex and have to be activated by vibronic coupling.[54] Note that the depolarization ratio of the band in question is 1/3,[27] suggesting that the 165 cm^{-1} mode is *totally* symmetric and is resonantly enhanced via a single nondegenerate electronic state.[55]

Recently, Hayashi et al. made ab initio calculations and a normal-mode analysis of the TCNE−HMB complex.[56] The scissoring mode of TCNE in the complex was calculated to be 167 cm^{-1} (b_{1u}),[57] and the TCNE out-of-plane bending mode was calculated to be 170 cm^{-1} (b_{3u}).[56,58]

The data concerning the frequencies of these two TCNE vibrations could be summarized as follows. Scissoring mode: (a) frequency is about 165 cm^{-1}; (b) there is no difference in frequency from the neutral to anion form; (c) it is nontotally symmetric in the complex. Out-of-plane bending mode: (a) frequency is about 165 cm^{-1} for neutral TCNE; (b) for the anion of TCNE the frequency is about 15 cm^{-1} smaller than that for the neutral form; (c) it is the totally symmetric mode in the complex. We think that the same vibrational mode that gives the peak in the Raman spectrum of the complex is responsible for the oscillations in the transient absorption and fluorescence experiments. There are two reasons which support the idea that this mode is the out-of-plane bending mode. (1) The frequency observed in the ground state of the complex (neutral TCNE; transient absorption (162 cm^{-1}) and resonance Raman (165 cm^{-1}) experiments) is larger than that observed in the excited state (anion of TCNE; fluorescence experiment(155 cm^{-1})). (2) The small depolarization ratio of 1/3 of the peak of interest observed in the resonance Raman spectrum of the complex suggests that the vibration is totally symmetric. Thus, we propose a new assignment of the oscillatory component and the Raman peak at 165 cm^{-1}, which is the out-of-plane bending mode of TCNE (b_{3u}).

TABLE 4: Selected Vibrations of Fluoranil (FlA) and Fluoranil Anion

	experimental	calculations			
	$\nu_{(FlA)}$/cm^{-1} from ref 59	$\nu_{(FlA)}$ cm^{-1}	$\nu_{(FlA^-)}$ cm^{-1}	species D_{2h}	description
ν_{14}	310	342	351/312[a]	b_{1u}	in-plane C−F bend
ν_{29}	217	234	230/206[a]	b_{3u}	out-of-plane C−F wag

[a] Value after slash was obtained by molecular orbital, density functional, and hybrid Hartree−Fock/density functional computations.[60]

4.6. Low-Frequency Vibrations of Fluoranil and Chloranil. For fluoranil, a strong IR absorption at about 217 cm^{-1} in chloroform was observed[59] and was assigned to the out-of-plane bending mode, ν_{29} (b_{3u}). The scissoring mode, ν_{14} (b_{1u}), which is also of interest has much higher frequency (310 cm^{-1}). No experimental data are available for the ν_{29} mode (b_{3u}) of fluoranil anion. The results of our semiempirical calculations as well as hybrid ab initio calculations[60] are shown in Table 4. From our calculations, about a 2% decrease of the frequency of the ν_{29} mode of fluoranil anion with respect to the neutral form was found, even though the absolute values of the calculated frequencies are overestimated. If we dare to use this calculated difference of 2% to get the frequency of the anion based on the experimental value for the neutral form of 217 cm^{-1}, we will get the value of 213 cm^{-1}. This is in good agreement with the experimental oscillatory frequency of 212 ± 7 cm^{-1} (Tables 1 and 4). So the observed oscillations in the fluoranil−HMB complex can be assigned to the out-of-plane bending mode, ν_{29} (b_{3u}), of fluoranil.

The peak at 186 cm^{-1} in the IR spectrum of chloranil was observed and assigned to the out-of-plane bending mode, ν_{29} (b_{3u}).[61] The scissoring mode, ν_{14} (b_{1u}), is probably obscured by the ν_{29} mode which is stronger.[61] No Raman-active modes were observed for chloranil around 178 cm^{-1}. The assignment of the ν_{29} mode (b_{3u}) of the anion of chloranil to 220 cm^{-1} [62] does not look reasonable, as a shift from the frequency of this mode from neutral chloranil is too large. The authors suggested that this value is probably influenced by a coupling with lattice modes.[62] From our calculations, a shift of about 2% to the lower frequencies for the ν_{29} (b_{3u}) mode is expected for anion of chloranil. The 2% correction of the 186 cm^{-1} experimental value (Table 5) gives the ν_{29} frequency of 182 cm^{-1} for anion. This value is in good agreement with the frequency of observed oscillations (179 ± 5 cm^{-1}). So we can assign the observed oscillations in the complexes with chloranil to the ν_{29} (b_{3u}) out-of-plane vibrational mode of chloranil. Thus, in the complexes with three acceptors studied, the oscillatory component is

TABLE 5: Selected Vibrations of Chloranil (ClA) and Chloranil Anion

	experimental		calculations			
	$\nu_{(ClA)}$/cm^{-1} ref 61	$\nu_{(ClA^-)}$/cm^{-1} refs 62,63	$\nu_{(ClA)}$ cm^{-1}	$\nu_{(ClA^-)}$ cm^{-1}	species D_{2h}	description
ν_{14}	(186)[a]	200	205	205/208[b]	b_{1u}	in-plane C−Cl bend
ν_{29}	186	220[c]	191	187/187[b]	b_{3u}	out-of-plane C−Cl wag

[a] The value is not well defined as it is probably obscured by the ν_{29}.[61] [b] Value after slash was obtained by molecular orbital, density functional, and hybrid Hartree−Fock/density functional computations.[60] [c] This mode is probably influenced by a coupling with lattice modes.[62]

assigned to the out-of-plane vibrational mode of the acceptors having the b_{3u} symmetry.

4.7. Intermolecular or Intermolecular? We think that upon photoexcitation of EDA complexes to the CT band, the intermolecular modes are excited as well as intramolecular modes since the equilibrium distance between D and A is altered in the ionic state of the complex. In this section, we are addressing a question, why the coherence due to the D−A stretching mode was not clearly observed in our experiments.

The value of the ground-state D−A stretching frequency is not well defined yet, but it probably is about 60[56] to 89 cm^{-1}.[48] In the excited state of the complex, one can expect some increase of the frequency of the D−A stretching mode due to the additional Coulombic attraction.[12] Two differences between the intermolecular D−A stretching mode and intramolecular modes could be stressed. First, an increase of the frequency is expected in the excited state of the complex for the D−A stretching mode, while the frequencies of intramolecular modes change very little. Particularly, the frequency of the b_{3u} out-of-plane mode of the acceptors slightly decrease in the excited state of the complex. Second, the shapes of the potential energy surface are different along inter- and intramolecular modes. The repulsive part of the potential is similar for both modes, but the attractive part is much less steep for the intermolecular mode (as it leads to dissociation of the complex), while for intramolecular modes the potential is rather symmetrical.

On the basis of these two differences, we suggest the possible reasons why it is difficult to observe the vibrational coherence due to the intermolecular mode. First, if the ground-state frequency is as small as 60−89 cm^{-1}, the thermal population of this mode at room temperature should be substantial. The fraction of vibrationally excited complexes $f(\upsilon=1)/f(\upsilon=0)$ is about 70%, where $f(\upsilon) = \exp(-\upsilon E_v/kT)$ is the Boltzmann function. If the vibrational mode is excited before photoexcitation, the initial phase at the moment of the excitation will be randomized arbitrarily. In other words, the initial D−A distance in the time of photoexcitation is not unique. This will make it difficult to observe the coherence caused by this vibration. Second, as the binding energy in the ground electronic state of the complex is not very large (about 14 kT for HMB−TCNE[30]), there is some distribution of binding energy. It results in some distribution of the frequency of the D−A stretching mode and possibly distribution of the D−A distance. Third, different types of intermolecular modes exist (not only the clear D−A stretching). Several D−A vibrational modes with frequencies of 41, 59, and 63 cm^{-1} were recently calculated for the ground state of the HMB−TCNE complex.[56] The peak at about 89 cm^{-1} was experimentally observed by Rossi et al.[48] for a microcrystalline sample of HMB−TCNE complex and was assigned to the D−A stretching mode. This peak is rather broad with a width of about 15−20 cm^{-1}, which is supporting the last two reasons. Thus, these effects should complicate the observation of the coherence of the D−A stretching mode.

Contrary to the intermolecular modes, the frequencies of intramolecular modes are less affected by solvent. The frequency of the intramolecular vibrations in the ground electronic state does not change much in the excited state. This frequency is much larger than the expected D−A stretching frequency, and it is less thermally populated (about 45% at room temperature). Thus, generally, it seems easier to observe coherence caused by the intramolecular mode than that caused by the D−A stretching mode in "weak" EDA complexes.

4.8. Modulation of the Mean Transition Moment by the b_{3u} Vibration. Another question could be asked. Why does the out-of-plane mode of the acceptor causes such strong oscillations and the in-plane scissoring mode having similar frequency does not? Two possible reasons for that could be discussed. One is trivial, the scissoring mode is not strongly excited in the optical transition (small FC factor). This is supported by Raman experiments with the complex where only one peak around 165 cm^{-1} is observed.[28,43,53,54] The second reason is an additional mechanism which causes oscillations. A modulation of the mean transition moment by the vibration is expected if oscillations are caused by the out-of-plane acceptor mode. We have discussed in section 4.2 that the wave packet motion in the excited state of the complex modulates the transition frequency. At the same time, the out-of-plane acceptor mode is strongly coupled to the transition moment, since it is directed toward the donor part and the vibrational motion modulates the distance between π systems of the donor and acceptor. In this case, one can expect modulation of the transition moment during the vibration. Then, the oscillations caused by this mode could be enhanced. A large modulation of the dipole moment by a vibration should modulate the fluorescence intensity. The mean electronic transition moment ($\bar{M}_{eg}(t)$) is estimated from the integral over absorption or fluorescence ($F(\nu,t)$) spectrum (eq 3).[64]

$$\bar{M}_{eg}{}^2(t) \approx S(t) = \int \frac{F(\nu,t)}{\nu^3} d\nu \qquad (3)$$

The $S(t)$ function is constructed by integration of the Gaussian fitting functions for the fluorescence spectra $F(\nu,t)$ at each time delay t. The result is shown in Figure 11. One can clearly see that the mean transition moment oscillates in time during the vibrations.

If the vibrational mode is strongly coupled to the transition moment, the enhancement of the Raman intensity can be expected. This is so-called the vibronic coupling effect which has been formalized by introducing the Herzberg−Teller expansion of electronic wave functions over vibrational modes.[65,66] If vibronic coupling is strong (simply speaking electronic wave functions change significantly during vibration) the Herzberg−Teller resonant term of the Raman scattering tensor becomes important in addition to the Franck−Condon term. We think that the b_{3u} mode of the acceptor is strong in Raman spectra of the HMB−TCNE complex due to the vibronic coupling mechanism. It should be noted that the out-of-plane mode of an acceptor is not out-of-plane mode in the complex.

The enhancement of IR activity in EDA complexes for the Raman-active modes of donors due to the vibronic coupling mechanism was observed for different complexes (for example,

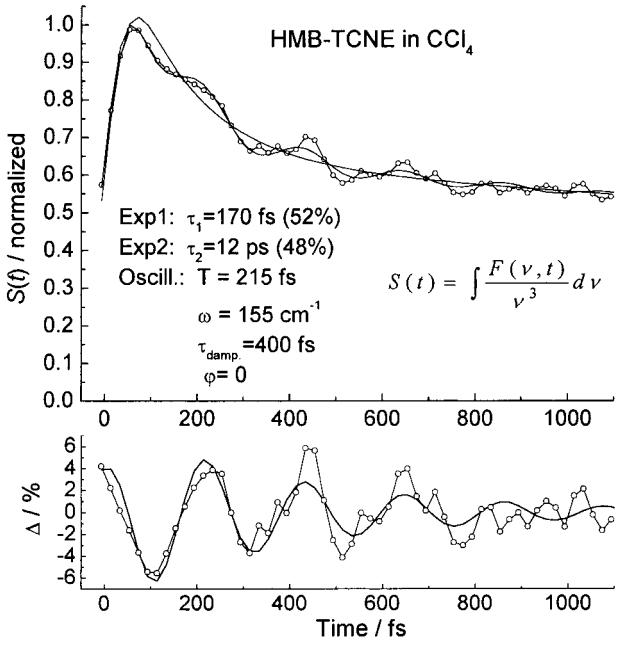

Figure 11. $S(t)$ function of time is shown which reflects modulation of the mean transition moment ($\bar{M}^2_{eg}(t)$) for HMB−TCNE complex in CCl_4. The parameters of the best fit by the $f(t)$ function (eq 1) are shown on the plot. The oscillating component is shown separately in the lower graph.

benzene−I_2,[67] ethylene−metallic cation[68]). It was shown that a small modulation of the transition moment by the vibration can increase significantly its IR activity.

The $S(t)$ function shows a fast decay component superimposed with oscillations (Figure 11). The biexponential fit of the $S(t)$ function (with oscillatory component) gives characteristic decay times of 170 fs and 12 ps. The latter value stands for the lifetime of the excited state and was fixed in the analysis. The fast decay component (∼170 fs) might be assigned to the fast recombination reaction from hot vibrational states as well as to a change of the transition moment during IVR and VR processes. Another possibility is to assign the fast decay component to a conversion between two CT excited states the presence of which was calculated in ref 56.

4.9. Phase of the Oscillations. It is experimentally shown that there are two mechanisms contributing to the observed coherent oscillations in fluorescence. One is the modulation of the transition frequency (spectral shift mechanism) and the other is modulation of the mean transition moment by the vibration. It is interesting to note that the initial phase of oscillations caused by the spectral shift mechanism depends on the wavelength of observation. A phase shift of π is expected for oscillations observed to the "red" from the fluorescence maximum compared with that observed to the "blue", while for wavelengths on the same side from the fluorescence maximum the initial phase is almost the same. The initial phase of oscillations caused by the mechanism of the transition moment modulation does not depend on the observed wavelengths. From Figures 3 and 11, one can see that at the "blue" slope of fluorescence spectrum, the oscillations caused by both mechanisms are in-phase. It is expected that on the "red" slope of fluorescence spectrum the oscillations caused by the two mechanisms are out-of-phase. As a result, oscillations at the "red" slope could be much smaller (if any). That could be the reason that almost no oscillations were observed in fluorescence at 970 nm for HMB−TCNE complex, which is to the "red" from the fluorescence maximum. This prediction need to be experimentally checked further more.

5. Conclusions

The spontaneous fluorescence of several EDA complexes shows oscillatory behavior superimposed with a fast decay component. The different frequencies of oscillations were observed for complexes with three different electron acceptors: tetracyanoethylene, fluoranil, and chloranil. Almost the same oscillatory frequency was observed for the complexes with different donors and a common acceptor in all three cases. These observations forced us to conclude that the intramolecular acceptor mode is responsible for the observed oscillations. Analysis of the existing far-IR and Raman spectra of the EDA complexes and acceptors allowed us to assign the out-of-plane bending mode of acceptors as the mode giving rise to oscillations in the spontaneous fluorescence for all three acceptors studied. To our knowledge, this is the most systematic assignment of the oscillatory mode made for such complicated molecular systems.

The out-of-plane bending mode of the acceptor is somewhat similar to the D−A stretching mode since the distance between the central π system of the acceptor and donor changes during vibration, although the center of mass of acceptor is not moving. It is shown that this mode is strongly coupled to the CT electronic transition and modulates the value of the transition moment. The modulation of the transition frequency by the vibration was shown by construction of the fluorescence peak shift correlation function.

Several conclusions are made on the assignment of the vibrational modes in the TCNE and HMB−TCNE complex. (1) The frequencies of the out-of-plane bending mode, ν_{14} (b_{3u}), of TCNE are expected to be ∼165 and ∼155 cm^{-1} for the ground and excited states, respectively. (2) The peak at 165 cm^{-1} in the IR spectra of TCNE is due to the out-of-plane bending mode, ν_{14} (b_{3u}). (3) The peak at 165 cm^{-1} in the Raman spectra of the HMB−TCNE complex is also mainly due to the out-of-plane bending mode of TCNE, ν_{14} (b_{3u}).

Acknowledgment. We acknowledge the financial support by a grant-in-aid (10440170) from the Ministry of Education, Science, Sports and Culture of Japan and the Inoue Science Foundation. We thank Prof. H. Hamaguchi of the University of Tokyo and Prof. S. Iwata of the Institute for Molecular Sciences for helpful discussions.

References and Notes

(1) Rosker, M. J.; Wise, F. W.; Tang, C. L. *Phys. Rev. Lett.* **1986**, *57*, 321.
(2) Rose, T. S.; Rosker, M. J.; Zewail, A. H. *J. Chem. Phys.* **1988**, *88*, 6672.
(3) Zewail, A. H. *Science* **1988**, *242*, 1645.
(4) Banin, U.; Ruhman, S. J. *Chem. Phys.* **1993**, *98*, 4391.
(5) Chesnoy, J.; Mokhtari, A. *Phys. Rev. A* **1988**, *38*, 3566.
(6) Okamoto, H.; Yoshihara, K., *Chem. Phys. Lett.* **1991**, *177*, 568.
(7) Lenderink, E.; Duppen, K.; Wiersma, D. A. *J. Phys. Chem.* **1995**, *99*, 8972.
(8) Voringer, P.; Westervelt, R. A.; Yang, T.-S.; Arnett, D. C.; Feldstein, M. J.; Scherer, N. F. *J. Raman Spectrosc.* **1995**, *26*, 535.
(9) Mokhtari, A.; Chebira, A.; Chesnoy, J. *J. Opt. Soc. B* **1990**, *7*, 1551.
(10) Hong, Q.; Pexton, I. A. D.; Porter, G.; Klug, D. R. *J. Phys. Chem.* **1993**, *97*, 12561.
(11) Seel, M.; Engleitner, S.; Zinth, W. *Chem. Phys. Lett.* **1997**, *275*, 363.
(12) Wynne, K.; Galli, C.; Hochstrasser, R. M. *J. Chem. Phys.* **1994**, *100*, 4797.
(13) Wynne, K.; Reid, G.; Hochstrasser, R. M. *J. Chem. Phys.* **1996**, *105*, 2287.
(14) Rubtsov, I. V.; Yoshihara, K. *J. Phys. Chem.* **1997**, *101*, 6138.
(15) Dunn, T. J.; Sweetser, J. N.; Walmsley, I. A. *Phys. Rev. Lett.* **1993**, *70*, 3388.

(16) Vos, M. H.; Rappaport, F.; Lambry, J.-C.; Breton, J.; Martin, J.-L. *Nature* **1993**, *363*, 320. Vos, M. H.; Lambry, J.-C.; Robles, S. J.; Youvan, D. C.; Breton, J.; Martin, J.-L. *Proc. Natl. Acad. Sci. U.S.A.* **1991**, *88*, 8885.
(17) Zhu, L.; Sage, J. T.; Champion, P. M. *Science* **1994**, *266*, 629.
(18) Bradforth, S. E.; Jimenez, R.; van Mourik, F.; van Grondelle, R.; Fleming, G. R. *J. Phys. Chem.* **1995**, *99*, 16179.
(19) Stanley, R. J.; Boxer, S. G. *J. Phys. Chem.* **1995**, *99*, 859.
(20) Vos, M. H.; Jones, M. R.; Martin, J.-L. *Chem. Phys.* **1998**, *223*, 179.
(21) Lim, M.; Wolford, M., F.; Hamm, P.; Hochstrasser, R. M.; *Chem. Phys. Lett.* **1998**, *290*, 355.
(22) Rubtsov, I. V.; Yoshihara, K. In *Ultrafast Phenomena XI*; Elsaesser, T., Fujimoto, J. G., Wiersma, D. A., Zinth, W., Eds.; Springer-Verlag: Berlin, 1998.
(23) Mulliken, R. S.; Person, W. B. *Molecular Complexes*; John Wiley & Sons: New York, 1969 and papers cited in it.
(24) Foster, R. *Organic charge-transfer complexes*; Academic Press: London, New York, 1969.
(25) Myers, A. B. *Chem. Rev.* **1996**, *96*, 911.
(26) Markel, F.; Ferris, N. S.; Gould, I. R.; Myers, A. B. *J. Am. Chem. Soc.* **1992**, *114*, 6208.
(27) Smith, M. L.; McHale, J. L. *J. Phys. Chem.* **1985**, *89*, 4002.
(28) Kulinowski, K.; Gould, I. R.; Myers, A. B. *J. Phys. Chem.* **1995**, *99*, 9017.
(29) Rubtsov, I. V.; Shirota, H.; Yoshihara, K. *J. Phys. Chem.* **1999**, *103*, 1801.
(30) Liptay, W.; Rehm, T.; Schanne, D. L.; Baumann, W.; Land, W. *Z. Naturforch. A* **1982**, *37*, 1427.
(31) (a) Foster, R.; Kulevsky, N. *J. Chem. Soc., Faraday Trans. 1* **1973**, *69*, 1427. (b) Frey, J. E.; Andrews, A. M.; Ankoviac, D. G.; Beaman, D. N.; Du Pont, L. E.; Elsner, T. E.; Lang, S. R.; Zwart, M. A. O.; Seagle, R. E.; Torreano, L. A. *J. Org. Chem.* **1990**, *55*, 606.
(32) Jean, J. *J. Chem. Phys.* **1994**, *101*, 10464.
(33) Jonas, D. M.; Bradforth, S. E.; Passino, S. A.; Fleming, G. R. *J. Phys. Chem.* **1995**, *99*, 2594.
(34) Unpublished simulations.
(35) Van der Zwan, G.; Hynes, J. T. *J. Phys. Chem.* **1985**, *89*, 4181.
(36) Bagchi, B.; Oxtoby, D. W.; Fleming, G. R. *Chem. Phys.* **1991**, *86*, 257.
(37) Simon, J. D. *Acc. Chem. Res.* **1988**, *21*, 128.
(38) Maroncelli, M.; MacInnis, J.; Fleming, G. R. *Science* **1988**, *243*, 1674.
(39) Kroll, M. *J. Am. Chem. Soc.* **1968**, *90*, 1097.
(40) Hanazaki, I. *J. Phys. Chem.* **1972**, *76*, 1982.
(41) Elsaesser, T.; Kaiser, W. *Annu. Rev. Phys. Chem.* **1991**, *42*, 83.
(42) Ashworth, S. H.; Hasche, T.; Woerner, M.; Riedle, E.; Elsaesser, T. *J. Phys. Chem.* **1996**, *100*, 5761.
(43) Kulinowski, K.; Gould, I. R.; Ferris, N. S.; Myers, A. B. *J. Phys. Chem.* **1995**, *99*, 17715.
(44) The excited state of the complex does not exactly corresponds to the case where the two unit charges are separated by the D−A distance. The dipole moment in the excited state in smaller than the one suggested by such a simple consideration (ref 31).
(45) TCNE has 24 fundamental vibrations which are classified as: $5a_g$(R) + $2a_u$(inactive) + b_{1g}(R) + $4b_{1u}$(IR) + $2b_{2g}$(R) + $4b_{2u}$(IR) + $4b_{3g}$(R) + $2b_{3u}$(IR), where (R) and (IR) indicate the Raman and infrared active modes, respectively.
(46) Though there is evidence for symmetric structure of the complexes of interest, the intermolecular forces are rather weak and allow a wide range of thermally accessible geometries in solution. For the case of lower symmetry of the complex (lower than C_2 group), no strict selection rules are held.
(47) Michaelian, K. H.; Rieckhoff, K. E.; Voigt, E. M. *J. Mol. Spectrosc.* **1982**, *95*, 1.
(48) Rossi, M.; Haselbach E. *Helv. Chim. Acta* **1979**, *62* (20), 140.
(49) Miller, F. A.; Sala, O.; Devling, P.; Overend, J.; Lippert, E.; Luder, E.; Moser, H.; Varchmin, J. *Spectrochim. Acta* **1964**, *20*, 1233.
(50) Iida, Y. *Bull. Chem. Soc. Jpn.* **1973**, *46*, 423.
(51) Stanley, J.; Smith, D.; Latimer, B.; Devlin, J. P. *J. Phys. Chem.* **1966**, *70*, 2011.
(52) Hinkel, J. J.; Devlin, J. P. *J. Chem. Phys.* **1973**, *58*, 4750.
(53) Jensen, P. W. *Chem. Phys. Lett.* **1977**, *45*, 415.
(54) McHale, J. L.; Merriam, M. J. *J. Phys. Chem.* **1989**, *93*, 526.
(55) Mortensen, O. S.; Hassing, S. *Adv. Infrared Raman Spectrosc.* **1980**, *6*, 1.
(56) Hayashi, M.; Yang, T.-S.; Yu, J.; Mebel, A.; Lin, S. H. *J. Phys. Chem. A* **1997**, *101*, 4156.
(57) We use the symmetry labels for acceptor vibrations in the complex in terms of the acceptor symmetry group (D_{2h}) for several reasons: (a) the complex is weak, so the vibrational modes are localized (modes in the complex localized on the acceptor are almost the same as on the acceptor itself); (b) it is much more informative to use this symmetry description than to describe them in terms of low symmetry complex; (c) the symmetry of the complex in solution is not well defined.
(58) Hayashi, M.; Yang, T.-S.; Yu, J.; Mebel, A.; Chang, R.; Lin, S. H.; Rubtsov, I. V.; Yoshihara, K. *J. Phys. Chem. A* **1998**, *102*, 4256.
(59) Girlando, A.; Pecile, C. *J. Chem. Soc., Faraday Trans. 2* **1975**, *71*, 689.
(60) Boesch, S. E.; Wheeler, R. A. *J. Phys. Chem.* **1997**, *101*, 8351.
(61) Girlando, A.; Pecile, C. *J. Chem. Soc., Faraday Trans. 2* **1973**, *69*, 1291.
(62) Girlando, A.; Zanon, I.; Bozio, R.; Pecile, C. *J. Chem. Phys.* **1978**, *68*, 22.
(63) Girlando, A.; Morelli, L.; Pecile, C. *Chem. Phys. Lett.* **1973**, *22*, 553.
(64) Birks, J. B. *Photophysics of Aromatic Molecules*; Wiley-Interscience: London, 1970.
(65) Albrecht, A. C. *J. Phys. Chem.* **1961**, *34*, 1476.
(66) For example, see: Nakamoto, K. *Infrared and Raman Spectra of Inorganic and Coordination Compounds*; Wiley-Interscience: New York, 1997.
(67) Ferguson, E. E. *J. Chem. Phys.* **1956**, *25*, 577.
(68) (a) Matsuzawa, H.; Yamashita, H.; Ito, M.; Iwata, S. *Chem. Phys.* **1990**, *147*, 77. (b) Matsuzawa, H.; Iwata, S. *Chem. Phys.* **1992**, *163*, 297.